



**HAL**  
open science

# Functional relation between growth, photosynthetic rate and regulation in the coastal picoeukaryote *Phaeomonas* sp. RCC 503 (Pinguiphyceae, Stramenopiles)

Vasco Giovagnetti, Maria Letizia Cataldo, Fabio Conversano, Christophe Brunet

## ► To cite this version:

Vasco Giovagnetti, Maria Letizia Cataldo, Fabio Conversano, Christophe Brunet. Functional relation between growth, photosynthetic rate and regulation in the coastal picoeukaryote *Phaeomonas* sp. RCC 503 (Pinguiphyceae, Stramenopiles). *Journal of Plankton Research*, 2010, 10.1093/plankt/FBQ074 . hal-00603440

**HAL Id: hal-00603440**

**<https://hal.science/hal-00603440>**

Submitted on 25 Jun 2011

**HAL** is a multi-disciplinary open access archive for the deposit and dissemination of scientific research documents, whether they are published or not. The documents may come from teaching and research institutions in France or abroad, or from public or private research centers.

L'archive ouverte pluridisciplinaire **HAL**, est destinée au dépôt et à la diffusion de documents scientifiques de niveau recherche, publiés ou non, émanant des établissements d'enseignement et de recherche français ou étrangers, des laboratoires publics ou privés.



**Functional relation between growth, photosynthetic rate  
and regulation in the coastal picoeukaryote *Phaeomonas* sp.  
RCC 503 (Pinguiphyceae, Stramenopiles)**

Journal:	<i>Journal of Plankton Research</i>
Manuscript ID:	JPR-2010-094.R1
Manuscript Type:	Original Article
Date Submitted by the Author:	27-May-2010
Complete List of Authors:	Giovagnetti, Vasco; Stazione Zoologica A. Dorhn, Laboratory of Ecology and Evolution of Plankton Cataldo, Maria Letizia; Stazione Zoologica A. Dorhn, Laboratory of Ecology and Evolution of Plankton Conversano, Fabio; Stazione Zoologica A. Dorhn, Laboratory of Ecology and Evolution of Plankton Brunet, Christophe; Stazione Zoologica A. Dorhn, Laboratory of Ecology and Evolution of Plankton
Keywords:	photoacclimation, picoeukaryote, xanthophyll cycle



1  
2  
3  
4 **Functional relation between growth, photosynthetic rate and**  
5 **regulation in the coastal picoeukaryote *Phaeomonas sp.* RCC**  
6 **503 (Pinguiphyceae, Stramenopiles)**  
7  
8  
9

10  
11  
12  
13  
14 **V. GIOVAGNETTI, M. L. CATALDO, F. CONVERSANO AND C. BRUNET\***  
15

16  
17  
18 Laboratory of Ecology and Evolution of Plankton, Stazione Zoologica Anton Dohrn, Villa  
19  
20 Comunale, 80121 Naples, Italy  
21  
22  
23

24  
25 \*: CORRESPONDING AUTHOR: christophe.brunet@szn.it  
26  
27  
28  
29

30 **Running head:** *Phaeomonas sp.* RCC 503 photoregulation and growth  
31  
32  
33  
34

35 **Key-words:** photoacclimation; picoeukaryote; xanthophyll cycle.  
36  
37  
38  
39

40 **Abbreviations:** Ax, antheraxanthin; DPS, de-epoxidation state [ $DPS = Z_x : (V_x + A_x +$   
41  $Z_x)$ ]; ETR, electron transport rate;  $F_v : F_m$ , PSII maximum photochemical efficiency;  
42 LHC, light-harvesting complex; Neox, neoxanthin; NPQ, non-photochemical quenching;  
43  
44 PAM, pulse amplitude modulation; PFD, photon flux density;  $V_x$ , violaxanthin;  $Z_x$ ,  
45  
46 zeaxanthin.  
47  
48  
49  
50  
51  
52  
53  
54  
55  
56  
57  
58  
59  
60

## ABSTRACT

Picoeukaryotes constitute good models for testing photophysiological hypotheses because of constraints as well as opportunities related to their minute size. This study was undertaken to investigate the relation between growth rate and regulation of photosynthesis in a coastal picoeukaryote, using the strain *Phaeomonas sp.* RCC 503 as a model. Here we address how photoacclimation responses affect photosynthetic capacity and how growth rate is modulated by photoacclimation and photosynthetic rate variations. Growth of the strain was followed over five days under five sinusoidal light regimes set to peak at maximal photon flux densities (PFD) of 10, 50, 100, 250 and 500  $\mu\text{mol photons m}^{-2} \text{ s}^{-1}$ . We measured growth rate, pigment composition, variable fluorescence, non-photochemical quenching, electron transport rate, absorption spectrum, cell carbon and nitrogen content one to three times per day under each of these five conditions. Results suggest that *Phaeomonas sp.* RCC 503 is a light-adapted species, showing a high physiological plasticity allowing it to grow under a broad range of PFD conditions. The PFD determined growth rate, the latter being correlated significantly to photosynthetic capacity. Biochemical properties of cells, in terms of carbon and nitrogen content were closely correlated to growth rate and PFD. Photoacclimation allows growth to be maintained at low irradiance except at 10  $\mu\text{mol photons m}^{-2} \text{ s}^{-1}$ , whereas photoprotection efficiency allows enhancement of growth at high PFDs.

## INTRODUCTION

In the field, maximum light intensity available for photosynthesis varies predictably over daily and annual cycles. Yet, superimposed on these cycles are such factors as cloud cover that affect the amount of incoming light in an unpredictable way. For phytoplankton, and especially coastal phytoplankton, mild turbulence of the water column adds even further to this unpredictability (Lewis *et al.*, 1984; MacIntyre *et al.*, 2000; Lichtman and Klausmeier, 2001); one moment a cell finds itself at depth where its photosystems must cope with low light intensity, whereas the next moment it may be transported up to the surface where its photosystems have to adjust itself rapidly to conditions approaching full sunlight.

Phytoplankton cells possess a number of physiological acclimation and regulatory responses to cope with these unpredictable, potentially extreme, and often rapid changes in light intensity (MacIntyre *et al.*, 2002; Raven and Geider, 2003).

Acclimation involves net synthesis or breakdown of macromolecules and so changes in pigment quota, stoichiometry of cell components, and ultrastructural changes in the cell. Regulation refers to faster processes than acclimatory ones (i.e. time constants of seconds to minutes) acting through the control of enzyme activities and energy dissipation pathways (Raven and Geider, 2003). Regulatory processes therefore allow photosynthesis to react instantaneously and reversibly the environmental changes occurring. These mechanisms include the Rubisco activity, state transition mechanism, and the xanthophyll cycle (Raven and Geider, 2003). The xanthophyll cycle (XC) is one of the main processes involved in the dissipation of excessively absorbed light energy through the non-photochemical quenching (NPQ, Finazzi *et al.*, 2006). In green algae and higher plants, and in other algal groups (i.e. Pinguiphyceae), the XC mechanism is based on the reversible de-epoxidation of violaxanthin (Vx) into zeaxanthin (Zx) through antheraxanthin (Ax). In most chlorophyll *c* (Chl *c*) containing phytoplankton species (e.g. Diatoms), it involves the inter-conversion between diadinoxanthin (Dd) and diatoxanthin (Dt; Stransky and Hager, 1970; Lavaud *et al.*, 2007; Dimier *et al.*, 2007 b). Accumulation of Zx or Dt is triggered by the formation of a pH gradient across the thylakoid membrane (e.g., see the review by Goss and Jakob, *in press*).

1  
2  
3 Little is known about the picoeukaryotes with respect to their ecophysiological features  
4 (Timmermans *et al.*, 2005; Dimier *et al.*, 2007 a, 2009; Six *et al.*, 2008, 2009). These  
5 small planktonic photolithotrophs usually dominate oligotrophic water ecosystems,  
6 reaching up to almost 50 percent of total biomass and production, while in eutrophic  
7 waters their contribution to the phytoplankton community is lower (Not *et al.*, 2005;  
8 Worden and Not, 2008). Their small size explains many of their biological and ecological  
9 features such as the large surface area per unit volume and the minimal diffusion  
10 boundary layer (i.e. higher nutrient consumption rates), the low sinking rate, the low  
11 packaging effect and the efficient light utilization (Raven, 1998; Raven *et al.*, 2005).

12 High plasticity in photosynthetic regulation has been described in picoeukaryotes. For  
13 instance, Six and collaborators (Six *et al.*, 2008, 2009) highlighted different  
14 photoacclimation strategies in three ecotypes of *Ostreococcus* related to their ecological  
15 niches. Intraspecific variability has been shown in *Pelagomomans calceolata* (Dimier *et*  
16 *al.*, 2009 a), demonstrating different photosynthetic regulation strategies in response to  
17 irradiance dynamics.

18 All these properties make picoeukaryotes interesting models for physiological studies  
19 aiming to analyze the functional responses of algae to environmental changes, and for  
20 instance to photon flux density (PFD) variability. The purpose of our experimentation  
21 was to investigate the relation between growth rate, photosynthetic capacity and  
22 photoacclimative process efficiency in the coastal picoeukaryote *Phaeomonas sp.* (strain  
23 RCC503, Pinguiphyceae, Stramenopiles). Physiological response curve (PRC, Peek *et*  
24 *al.*, 2002) experiments were performed plotting physiological variables and growth rate  
25 against a range of PFD. The questions behind this work were: what kind of  
26 photoresponses are developed by this species when low and high light conditions are  
27 experienced? How do these responses explain photosynthetic efficiency changes?

28 Population growth was investigated over five days under five different sinusoidal light  
29 regimes set to peak at maximal photon flux densities of 10, 50, 100, 250 and 500  $\mu\text{mol}$   
30  $\text{photons m}^{-2} \text{s}^{-1}$ . Pigments, variable fluorescence, NPQ, electron transport rate, absorption  
31 spectra, cell carbon and nitrogen content together with size, volume and cell  
32 concentrations were measured one to three times per day during the exponential phase.  
33  
34  
35  
36  
37  
38  
39  
40  
41  
42  
43  
44  
45  
46  
47  
48  
49  
50  
51  
52  
53  
54  
55  
56  
57  
58  
59  
60

## METHOD

### Algal model and culture conditions

The strain RCC503 of *Phaeomonas sp.* (Pinguiphyceae) was isolated along the Mediterranean Spanish coast and was provided by the Roscoff Culture Collection (Vaulot *et al.*, 2004). The strain was cultivated nonaxenically at 20 °C at 100  $\mu\text{mol photons m}^{-2} \text{s}^{-1}$  with a 11:13 hours light : dark photoperiod in locally obtained, and sterilized seawater amended with f/2 medium (Guillard and Ryther, 1962) using 225  $\text{cm}^2$  polystyrene canted-neck flasks (Corning Incorporated, NY, 14831, USA). Cultures were continuously aerated and maintained in exponential phase by daily and semi-continuous dilution (50% of the total volume) over a period of more than two weeks before the experiments. Before performing experiments, we checked pre-acclimation of the strain to the light condition, by assessing stability of pigment content and growth rate.

### Experimental design and sampling strategy

After 15 days acclimation period at 100  $\mu\text{mol photons m}^{-2} \text{s}^{-1}$ , cultures were subjected to 5 different sinusoidal light (SL, Fig. 1a) regimes, each with a different maximal photon flux density (PFD) of 10 (LL1), 50 (LL2), 100 (ML), 250 (HL1), 500 (HL2)  $\mu\text{mol photons m}^{-2} \text{s}^{-1}$ , respectively. The mean PFD over the 11 h of illumination ranged between 344 and 7  $\mu\text{mol photons m}^{-2} \text{s}^{-1}$ , which is likely similar to the light experienced by cells at a depth of 10 m and at the Deep-Chlorophyll maximum layer in a Mediterranean water column, respectively (see Dimier *et al.*, 2009 a).

Population growth was followed over five days while photophysiological and biochemical properties of *Phaeomonas sp.* were measured during the exponential growth phase. Under the LL conditions, where no exponential phase was observed, sampling of photophysiological and biochemical parameters lasted five days.

Each experiment was performed in triplicate. Flasks were illuminated by the light-bulb kit ACLS (Advanced Control Lighting System) and Infinity XR4 (Aquarium Technologies - Sfiligoi S.r.l., Bassano del Grappa, Italy), simulating light-dark sinusoidal cycles, reproducing dawn and sunset. XR4 is equipped with metallic iodur HQI bulbs

(10000° K). PFD was measured with a 4π quantummeter (sensor QSL 2101, Biospherical Instruments Inc., San Diego, CA, USA).

Cultures were sampled three times per day (Fig. 1a). First sampling was carried out during dawn (for HL2 condition, incident irradiance was below 40 μmol photons m<sup>-2</sup> s<sup>-1</sup>), while the second corresponded with the irradiance peak. The third one was carried out during sunset (HL2 incident irradiance was below 40 μmol photons m<sup>-2</sup> s<sup>-1</sup>). Twenty to fifty milliliters of culture were rapidly taken with a 50 mL syringe during each sampling time, for measuring variable fluorescence, NPQ, electron transport rate, and for further analysis of pigments, absorption spectrum, cell size and volume (by Coulter Counter analysis) and cell concentrations (by microscopic counts).

Temperature and pH were controlled daily with a HI-9214-Stick pH meter (Hanna Instruments, Woonsocket, RI, USA). The growth rate was estimated daily from cell abundance measurements using the following equation:

$$\mu = \ln [N_{t_2} : N_{t_1}] : [t_2 - t_1] \quad (1)$$

where  $\mu$  is the growth rate (d<sup>-1</sup>) and  $N_t$  is the mean cell concentration at time  $t$ , where  $t_1$  and  $t_2$  correspond to the morning sampling time of days 1 and 2, respectively. From the growth rate, the number of cell divisions ( $n$ ) per day was estimated with the following equation:

$$n = \mu : [\ln(2)] \quad (2)$$

where  $n$  is the number of cell divisions per day and  $\mu$  is the growth rate.

### Pigment analysis

One aliquot of algal culture (10 mL) was filtered onto GF/F glass-fiber filters (Whatman) and immediately stored in liquid nitrogen until analysis. Triplicate samples were taken during each sampling time. Analysis was carried out following the procedure described in Dimier *et al.* (2007 a). The pigment extract was injected in a Hewlett Packard series 1100 HPLC (Hewlett-Packard) with a C8 BDS 3 mm Hypersil, IP column (Thermo Electron).

The mobile phase was composed of two solvent mixtures: methanol and aqueous ammonium acetate (70:30) and methanol. Pigments were detected spectrophotometrically at 440 nm using a Model DAD, Series 1100 Hewlett Packard photodiode array detector. Fluorescent pigments were detected in a Hewlett Packard standard FLD cell series 1100 with excitation and emission wavelengths set at 407 and 665 nm, respectively. Determination and quantification of pigments used pigment standards from D.H.I. Water & Environment (Hørsholm, Denmark).

### Variable fluorescence and NPQ

Only during the irradiance peak sampling time were samples for PAM measurements taken. Photochemical efficiency of PSII was estimated by a Phyto-PAM fluorometer (Heinz Walz GmbH, Effeltrich, Germany). Triplicate measurements of variable fluorescence were performed on both light- and 15-min dark- acclimated samples. The maximum photochemical efficiency ( $F_v : F_m$ , with  $F_v = F_m - F_o$ ) was measured on 15-min dark-acclimated sample during the irradiance peak sampling time.  $F_m$  and  $F_m'$  were measured after a saturating pulse of red light ( $2400 \mu\text{mol photons m}^{-2} \text{s}^{-1}$  for 450 ms) causing a complete reduction of the PSII acceptor pool.

The non-photochemical quenching of fluorescence was quantified by the Stern-Volmer expression:

$$\text{NPQ} = (F_m : F_m') - 1 \quad (3)$$

Electron transport rate (ETR) vs. light curves were determined on 15-min dark-exposed samples applying ten increasing irradiances ( $I$  from 1 to  $1500 \mu\text{mol photons m}^{-2} \text{s}^{-1}$ , for 2 min each). The absolute Electron Transport Rate (expressed in  $e^- \text{ Chl } a^{-1} \text{ h}^{-1}$ ) was calculated as follows:

$$\text{absETR} = (F_v' : F_m') \cdot I \cdot (a^*_{\text{ph}} : 2) \quad (4)$$

1  
2  
3 where  $I$  is the incident irradiance (in  $\mu\text{mol photons m}^{-2} \text{ s}^{-1}$ ). The mean absorption value  
4 ( $a^*_{\text{ph}}$ ) of phytoplankton was normalized by Chl  $a$  ( $\text{m}^2 \text{ mg Chl } a^{-1}$ ) and divided by 2  
5  
6 assuming that half of the absorbed light was distributed to PSII.

7  
8 The ETR-light curves were fitted with the equation of Eilers and Peeters (1988) to  
9  
10 estimate the photosynthetic parameters  $\alpha^{\text{B}}$ ,  $E_{\text{k, abs}} \text{ETR}_{\text{max}}$ . The relative Electron Transport  
11  
12 Rate ( $_{\text{rel}}\text{ETR}_{\text{max}}$ ) was estimated with equation (4) without Chl  $a$  normalization.

### 13 14 15 16 **Organic Carbon and Nitrogen**

17 Samples for the determination of particulate organic carbon (POC) and particulate  
18  
19 organic nitrogen (PON) were filtered on pre-combusted ( $450^\circ\text{C}$ , 5h) glass fiber filters  
20  
21 (Whatman GF/F) and immediately stored at  $-20^\circ\text{C}$ . The analyses were performed with a  
22  
23 FlashEA 1112 Series Thermo Electron CHN elemental analyzer (Hedges and Stern,  
24  
25 1984). Cyclohexanone-2,4-dinitrophenyl hydrazone was used as standard.

### 26 27 28 **Absorption spectrum**

29 Ten milliliter sample were filtered onto Whatman GF/F filters and immediately frozen.  
30  
31 Measurements were carried out following the procedure described in Dimier *et al.* (2007  
32  
33 a). Absorption was measured between 280 nm and 800 nm with 1-nm increments on a  
34  
35 spectrophotometer (Hewlett Packard HP-8453E) equipped with an integrating sphere  
36  
37 (Labsphere RSA-HP-53). The mean absorption value ( $a^*$ ) was thus normalized by the  
38  
39 Chl  $a$  concentration of the sample to obtain the Chl  $a$  specific absorption coefficient  
40  
41 ( $a^*_{\text{ph}}$ ,  $\text{m}^2 \text{ mg Chl } a^{-1}$ ).

## 42 43 44 **RESULTS**

### 45 46 47 **Growth**

48  
49 *Phaeomonas sp.* was able to grow under the entire range of light conditions with the  
50  
51 exception of LL1 ( $10 \mu\text{mol photons m}^{-2} \text{ s}^{-1}$ ) and showed the highest growth rate under the  
52  
53 highest light regime (Fig. 1b). At the end of the exponential phase for the HL and ML  
54  
55 conditions or at day 5 for LL conditions, where no exponential phase was found, cell  
56  
57 concentrations ranged between  $1.77 \times 10^4 \pm 1.98 \times 10^3$  and  $3.66 \times 10^5 \pm 9.15 \times 10^4$  cells  
58  
59  
60

1  
2  
3 mL<sup>-1</sup> following a positive light gradient. Number of divisions per day ranged between 0  
4 and 0.44 d<sup>-1</sup>. Cell size and volume were 3.27 ± 0.07 μm and 18.65 ± 0.95 μm<sup>3</sup>,  
5  
6 respectively. Only under the lowest PFD, did cells show a decrease of size and volume  
7  
8 (2.86 ± 0.02 μm and 12.28 ± 0.19 μm<sup>3</sup>).  
9

### 10 11 12 **Photosynthetic pigments**

13 Together with Chl *a*, many accessory pigments were present in the LHCs of *Phaeomonas*  
14 *sp.* and the main ones were the following: chlorophyll (Chl) *c*<sub>2</sub>, fucoxanthin (Fuco), cis-  
15 fucoxanthin (*cis*-Fuco), neoxanthin (Neox), Chl *c*<sub>3</sub> and β-carotene (β-Car).  
16  
17

18 The mean Chl *a* content per cell was significantly higher in LL conditions compared to  
19 the ML or HL ones ranging between 9.96 × 10<sup>-17</sup> ± 1.93 × 10<sup>-17</sup> and 2.82 × 10<sup>-16</sup> ± 7.13 ×  
20 10<sup>-17</sup> mol Chl *a* cell<sup>-1</sup> (Fig. 2a). It can be seen that a higher Chl *a* cell<sup>-1</sup> value was  
21 measured under HL2 relative to HL1.  
22

23 Lowering of the light harvesting capacity under high light was revealed by the decrease  
24 of almost all main accessory pigments (Fig. 2b, c), in agreement with the lower Chl *a*  
25 specific absorption coefficient (a\*<sub>ph</sub>, data not shown). Following their distribution over  
26 the different PFD gradient, three groups of accessory pigments could be defined. The first  
27 group was formed by Chl *c*<sub>2</sub> and fucoxanthin (Fig. 2b and c, respectively) as well as  
28 violaxanthin and antheraxanthin (see xanthophyll cycle paragraph) showing similar  
29 values at LL1 and LL2. Minor pigments such as Chl *c*<sub>3</sub>, cis-fucoxanthin and β-carotene  
30 (Fig. 2b and c, respectively) belonged to the second group characterized by an increase  
31 from LL2 to LL1, as the Chl *a* pool. Pigments of the third group (neoxanthin and  
32 zeaxanthin, Figs. 2d and 6b, respectively) showed a strong increase under HL conditions.  
33  
34 The uncoupling between Chl *a* and the main photosynthetic accessory pigments in  
35 response to light change could be a signal of a special photoacclimative strategy  
36 developed by this species under low light stress.  
37  
38  
39  
40  
41  
42  
43  
44  
45  
46  
47  
48  
49

### 50 51 **Organic Carbon and Nitrogen**

52 Cellular carbon and nitrogen concentrations were significantly correlated (p<0.001) and  
53 both strongly related to PFD regimes with lower concentrations under high light and  
54 vice-versa (Fig. 3a).  
55  
56  
57  
58  
59  
60

1  
2  
3 The Chl *a* : POC ratio varied slightly, increasing a little from LL to HL regimes (Fig. 3b),  
4 mainly due to the decrease of POC along the light gradient.  
5

6  
7 The POC : PON ratio, ranging between  $4.80 \pm 0.24$  and  $6.82 \pm 0.08$ , increased from low  
8 to high PFD regime (Fig. 3c) and was significantly correlated to growth rate ( $r^2 = 0.98$ ,  
9 Fig. 3d).  
10  
11

### 12 13 14 **Photosynthetic parameters**

15 The maximal photosynthetic rate ( $_{\text{abs}}\text{ETR}_{\text{max}}$ ) increased from the LL to HL regimes,  
16 reaching a maximum at HL1 and then decreasing a little under HL2 (Fig. 4a). A  
17 significantly correlated trend between  $_{\text{abs}}\text{ETR}_{\text{max}}$  and growth rate was observed (Fig. 4b).  
18 Under HL2, Chl *a* enhancement without any related increase in electron transport rate  
19 prevented this light condition fitting a linear regression. Indeed, when ETR was not  
20 reported in relation to Chl *a* concentration, the relationship between  $_{\text{rel}}\text{ETR}_{\text{max}}$  and growth  
21 rate was highly significant and linear over all the PFD range ( $r^2 = 0.92$ ; Fig. 4c).  
22  
23

24 The photosynthetic efficiency ( $\alpha^{\text{B}}$ , Fig. 4d) showed a maximum under the ML condition  
25 in agreement with the  $100 \mu\text{mol photons m}^{-2} \text{s}^{-1}$  pre-acclimation period of cells, and  
26 decreased with higher PFDs. Low values of  $\alpha^{\text{B}}$  under low LL1 and LL2 (similar to the  
27 HL1 and HL2 ones) might reflect a limited capacity for photosynthetic acclimation at  
28 low PFDs. Indeed, the light saturation index ( $E_k$ ) did not decrease under the value of  $200$   
29  $\mu\text{mol photons m}^{-2} \text{s}^{-1}$ , whereas it increased to almost  $1000 \mu\text{mol photons m}^{-2} \text{s}^{-1}$   
30 in agreement with the light-acclimated state of this species (Fig. 4e). The high values of  $E_k$   
31 indicated that cells were subjected to limiting or sub-optimal irradiance during light  
32 periods in all the five experimental conditions. The amplitude of light limitation,  
33 estimated with the  $E_k$  : PFD ratio, ranged between 24 and 2 (Fig. 4f), with LL1 and LL2  
34 having values higher than 10.  
35  
36  
37  
38  
39  
40  
41  
42  
43  
44  
45  
46  
47  
48

### 49 **Photophysiology and the xanthophyll cycle**

50 The PSII maximum photochemical efficiency ( $F_v$  :  $F_m$ ) showed a small range of  
51 variation, with the highest value under LL1 (0.61, Fig. 5a) and the lowest under HL1  
52 (0.56,  $250 \mu\text{mol photons m}^{-2} \text{s}^{-1}$ ). Under HL1 and HL2, *Phaeomonas sp.* developed non-  
53  
54  
55  
56  
57  
58  
59  
60

1  
2  
3 photochemical quenching (Fig. 5b), while it did not under lower PFD regimes, with the  
4 exception of LL1.  
5

6  
7 A significant linear correlation was found between NPQ and the photoprotective pigment  
8 zeaxanthin [ $Zx : (Vx + Ax + Zx)$ ], suggesting a relevant role of  $Zx$  in the development of  
9 NPQ in *Phaeomonas sp.* (Fig. 6a).  $Zx$  contribution to the xanthophyll cycle was low (less  
10 than 10%) revealing the limited need for photoprotection, in relation with the gradual  
11 PFD increase and the not so extreme irradiance peak applied during the experimental  
12 conditions.  
13  
14

15  
16  
17 The highest values of  $Zx$  were found in cultures grown under HL1 and HL2 (Fig. 6b).  
18 The two pigments  $Vx$  and  $Ax$ , expressed per cell (data not shown), followed the same  
19 trend of Chl *a* and other accessory photosynthetic pigments  $\text{cell}^{-1}$  (see Fig. 2).  
20

21 Daily evolution of  $Zx$  (Fig. 6c) showed that only under the HL2 condition did this  
22 pigment increase significantly at midday. Even though NPQ was similar between the two  
23 HLs,  $Zx$  concentration differed between the two conditions suggesting that a proportion  
24 of zeaxanthin was not involved in NPQ development. The morning value of  $Zx$  under the  
25 HL2 regime was higher than the values measured during each of the HL1 sampling times,  
26 revealing a daily-persisting photoprotective state.  
27  
28  
29  
30  
31  
32

## 33 34 35 **DISCUSSION**

36  
37  
38 Chl *a* content in *Phaeomonas sp.* RCC503 ( $\sim 2 \times 10^{-16}$  mol Chl *a*  $\text{cell}^{-1}$ , cell size  $\sim 3.3$   
39  $\mu\text{m}$ ) is in the range of values measured in other small size algal species (Dimier *et al.*,  
40 2007, 2009 b). Combining this study with data from Dimier *et al.* (2009 b), a highly  
41 significant correlation between size and Chl *a*  $\text{cell}^{-1}$  content was obtained (6 species with  
42 size ranged between 1.8 and 4.0  $\mu\text{m}$ ,  $r^2 = 0.92$ ) proving the direct relevance of size in  
43 determining pigment content in small species. Taxonomical difference does not affect the  
44 relation between size and Chl *a*, while processes such as photoacclimation have a small  
45 effect on this relation in picoeukaryotes (Dimier *et al.*, 2009 b, this study). Indeed,  
46 variations in cell size are so small over the irradiance range that any allometric effect (see  
47 Finkel *et al.*, 2010) becomes undetectable.  
48  
49

50  
51  
52  
53  
54  
55  
56  
57  
58  
59  
60  
61  
62  
63  
64  
65  
66  
67  
68  
69  
70  
71  
72  
73  
74  
75  
76  
77  
78  
79  
80  
81  
82  
83  
84  
85  
86  
87  
88  
89  
90  
91  
92  
93  
94  
95  
96  
97  
98  
99  
100  
101  
102  
103  
104  
105  
106  
107  
108  
109  
110  
111  
112  
113  
114  
115  
116  
117  
118  
119  
120  
121  
122  
123  
124  
125  
126  
127  
128  
129  
130  
131  
132  
133  
134  
135  
136  
137  
138  
139  
140  
141  
142  
143  
144  
145  
146  
147  
148  
149  
150  
151  
152  
153  
154  
155  
156  
157  
158  
159  
160  
161  
162  
163  
164  
165  
166  
167  
168  
169  
170  
171  
172  
173  
174  
175  
176  
177  
178  
179  
180  
181  
182  
183  
184  
185  
186  
187  
188  
189  
190  
191  
192  
193  
194  
195  
196  
197  
198  
199  
200  
201  
202  
203  
204  
205  
206  
207  
208  
209  
210  
211  
212  
213  
214  
215  
216  
217  
218  
219  
220  
221  
222  
223  
224  
225  
226  
227  
228  
229  
230  
231  
232  
233  
234  
235  
236  
237  
238  
239  
240  
241  
242  
243  
244  
245  
246  
247  
248  
249  
250  
251  
252  
253  
254  
255  
256  
257  
258  
259  
260  
261  
262  
263  
264  
265  
266  
267  
268  
269  
270  
271  
272  
273  
274  
275  
276  
277  
278  
279  
280  
281  
282  
283  
284  
285  
286  
287  
288  
289  
290  
291  
292  
293  
294  
295  
296  
297  
298  
299  
300  
301  
302  
303  
304  
305  
306  
307  
308  
309  
310  
311  
312  
313  
314  
315  
316  
317  
318  
319  
320  
321  
322  
323  
324  
325  
326  
327  
328  
329  
330  
331  
332  
333  
334  
335  
336  
337  
338  
339  
340  
341  
342  
343  
344  
345  
346  
347  
348  
349  
350  
351  
352  
353  
354  
355  
356  
357  
358  
359  
360  
361  
362  
363  
364  
365  
366  
367  
368  
369  
370  
371  
372  
373  
374  
375  
376  
377  
378  
379  
380  
381  
382  
383  
384  
385  
386  
387  
388  
389  
390  
391  
392  
393  
394  
395  
396  
397  
398  
399  
400  
401  
402  
403  
404  
405  
406  
407  
408  
409  
410  
411  
412  
413  
414  
415  
416  
417  
418  
419  
420  
421  
422  
423  
424  
425  
426  
427  
428  
429  
430  
431  
432  
433  
434  
435  
436  
437  
438  
439  
440  
441  
442  
443  
444  
445  
446  
447  
448  
449  
450  
451  
452  
453  
454  
455  
456  
457  
458  
459  
460  
461  
462  
463  
464  
465  
466  
467  
468  
469  
470  
471  
472  
473  
474  
475  
476  
477  
478  
479  
480  
481  
482  
483  
484  
485  
486  
487  
488  
489  
490  
491  
492  
493  
494  
495  
496  
497  
498  
499  
500  
501  
502  
503  
504  
505  
506  
507  
508  
509  
510  
511  
512  
513  
514  
515  
516  
517  
518  
519  
520  
521  
522  
523  
524  
525  
526  
527  
528  
529  
530  
531  
532  
533  
534  
535  
536  
537  
538  
539  
540  
541  
542  
543  
544  
545  
546  
547  
548  
549  
550  
551  
552  
553  
554  
555  
556  
557  
558  
559  
560  
561  
562  
563  
564  
565  
566  
567  
568  
569  
570  
571  
572  
573  
574  
575  
576  
577  
578  
579  
580  
581  
582  
583  
584  
585  
586  
587  
588  
589  
590  
591  
592  
593  
594  
595  
596  
597  
598  
599  
600  
601  
602  
603  
604  
605  
606  
607  
608  
609  
610  
611  
612  
613  
614  
615  
616  
617  
618  
619  
620  
621  
622  
623  
624  
625  
626  
627  
628  
629  
630  
631  
632  
633  
634  
635  
636  
637  
638  
639  
640  
641  
642  
643  
644  
645  
646  
647  
648  
649  
650  
651  
652  
653  
654  
655  
656  
657  
658  
659  
660  
661  
662  
663  
664  
665  
666  
667  
668  
669  
670  
671  
672  
673  
674  
675  
676  
677  
678  
679  
680  
681  
682  
683  
684  
685  
686  
687  
688  
689  
690  
691  
692  
693  
694  
695  
696  
697  
698  
699  
700  
701  
702  
703  
704  
705  
706  
707  
708  
709  
710  
711  
712  
713  
714  
715  
716  
717  
718  
719  
720  
721  
722  
723  
724  
725  
726  
727  
728  
729  
730  
731  
732  
733  
734  
735  
736  
737  
738  
739  
740  
741  
742  
743  
744  
745  
746  
747  
748  
749  
750  
751  
752  
753  
754  
755  
756  
757  
758  
759  
760  
761  
762  
763  
764  
765  
766  
767  
768  
769  
770  
771  
772  
773  
774  
775  
776  
777  
778  
779  
780  
781  
782  
783  
784  
785  
786  
787  
788  
789  
790  
791  
792  
793  
794  
795  
796  
797  
798  
799  
800  
801  
802  
803  
804  
805  
806  
807  
808  
809  
810  
811  
812  
813  
814  
815  
816  
817  
818  
819  
820  
821  
822  
823  
824  
825  
826  
827  
828  
829  
830  
831  
832  
833  
834  
835  
836  
837  
838  
839  
840  
841  
842  
843  
844  
845  
846  
847  
848  
849  
850  
851  
852  
853  
854  
855  
856  
857  
858  
859  
860  
861  
862  
863  
864  
865  
866  
867  
868  
869  
870  
871  
872  
873  
874  
875  
876  
877  
878  
879  
880  
881  
882  
883  
884  
885  
886  
887  
888  
889  
890  
891  
892  
893  
894  
895  
896  
897  
898  
899  
900  
901  
902  
903  
904  
905  
906  
907  
908  
909  
910  
911  
912  
913  
914  
915  
916  
917  
918  
919  
920  
921  
922  
923  
924  
925  
926  
927  
928  
929  
930  
931  
932  
933  
934  
935  
936  
937  
938  
939  
940  
941  
942  
943  
944  
945  
946  
947  
948  
949  
950  
951  
952  
953  
954  
955  
956  
957  
958  
959  
960  
961  
962  
963  
964  
965  
966  
967  
968  
969  
970  
971  
972  
973  
974  
975  
976  
977  
978  
979  
980  
981  
982  
983  
984  
985  
986  
987  
988  
989  
990  
991  
992  
993  
994  
995  
996  
997  
998  
999  
1000

1  
2  
3 adequately cope with different light environments thanks to efficient photoacclimative  
4 processes concerning both cell physiology and biochemistry. This is consistent with its  
5 origin from a Mediterranean coastal area, i.e. adapted to grow under variable light  
6 conditions.  
7  
8

9  
10 Increase in Chl  $c_3$  under low light has been found in many species both in laboratory  
11 (Rodriguez *et al.*, 2006; Dimier *et al.*, 2009 a) and in field experiments, where higher Chl  
12  $c_3$  values were found in the Deep-Chlorophyll Maximum layer (Brunet *et al.*, 2007), in  
13 agreement with its efficient role in light harvesting (Johnsen and Sakshaug, 1993). Thus,  
14 our study reinforces the hypothesis of a photoacclimative role of this pigment and  
15 demonstrates that changes in Chl  $c_3$  are independent of other pigments, such as  
16 fucoxanthin, Chl  $c_2$  and Chl  $a$ . Since Chl  $c_3$  is broadly present in phytoplankton species,  
17 and in many picoeukaryotes, this result would need further investigation to understand  
18 the ecological advantage in synthesizing such a pigment and how its synthetic pathway  
19 would work.  
20  
21

22 The significant relation between photosynthetic rate, cell biochemistry changes and  
23 growth rate suggests a direct and functional link between PFD, photoacclimation,  
24 photosynthetic and growth rate. In many studies, the variability of the relationship  
25 between photosynthetic organic matter production and cell growth has been highlighted  
26 (Litchman, 2000), growth and photosynthetic parameters being poorly coupled (van  
27 Leeuwe *et al.*, 2005). This variability has been attributed to factors such as variations in  
28 respiration rates, dissolved organic matter loss from cells, and changed extent of  
29 metabolites storage such as polysaccharides (van Leeuwe *et al.*, 2005).  
30  
31

32 The observed result is probably linked to the experimental conditions we applied.  
33 Simulating what occurs in nature, the sinusoidal irradiance evolution causes cells to  
34 experience a low or moderate daily-integrated PFD with a short irradiance peak. Our  
35 experimental conditions prevented either continuous high light or continuous limited light  
36 stress as occurs under quadratic light evolution. Small cell size limits the intracellular  
37 storage of energy (Raven, 1998) that might enhance the coupling of photosynthesis and  
38 growth rate, as already discussed by Dimier *et al.* (2009 a) for the picoeukaryote  
39 *Pelagomonas calceolata*.  
40  
41  
42  
43  
44  
45  
46  
47  
48  
49  
50  
51  
52  
53  
54  
55  
56  
57  
58  
59  
60

1  
2  
3 Growth rate is linearly related to both  $E_k$  : PFD ( $r^2 = 0.96$ ,  $p < 0.001$ ) and the POC : PON  
4 ratio ( $r^2 = 0.98$ ,  $p < 0.001$ ), these two ratios being correlated ( $r^2 = 0.95$ ,  $p < 0.001$ ). These  
5 results indicate a functional and linear link between PFD and growth rate through  
6 photosynthetic rate adjustments and consequently changes in cellular biochemistry. The  
7 great range of variation of the POC : PON ratio (35%, between 4.80 to 6.50) reveals  
8 significant biochemical modifications related to irradiance and growth rate variations  
9 (e.g., Finkel *et al.*, 2010).

10  
11 Higher values of POC : PON obtained under the higher PFD conditions are close to the  
12 Redfield ratio, a result that led us to reinforce the hypothesis of an optimal physiological  
13 state of cells under high light.

14  
15 Growth rate being the highest under HL2 condition, the photoacclimative strategy  
16 adopted by *Phaeomonas sp.* is efficient. This species belongs to the “light adapted”  
17 functional category (Falkowski and Owens, 1980; Falkowski, 1983), as also suggested by  
18 the high light saturation for photosynthesis ( $E_k$ ) estimated from the ETR-light curves.  
19 Under the HL2 condition, the small decrease of maximal photosynthetic rate per Chl *a*  
20 unit ( $_{\text{abs}}\text{ETR}_{\text{max}}$ ) compared to the HL1 condition while growth rate still increased  
21 relatively could be due to the Chl *a* cell<sup>-1</sup> increase. Indeed, the relation between  $_{\text{rel}}\text{ETR}_{\text{max}}$   
22 and growth rate is linear over the light gradient (Fig. 4c). Increase in both Chl *a* and  
23 accessory photosynthetic pigments under the HL2 condition suggests the development of  
24 a  $\sigma$ -type photoacclimation strategy aiming to increase the size of light harvesting  
25 antennae (Six *et al.*, 2008, Dimier *et al.*, 2009 a). Increase in photosynthetic pigments  
26 under the highest PFD condition was surprising since cells developed photoprotection  
27 when irradiance reached its maximum. Comparison with HL1 condition, where no  
28 pigment increase was noticeable, pigment enhancement under HL2 condition might be  
29 related to the strongest photoprotection. Both the higher level of Zx and its persistent  
30 presence in cells growing under the HL2 condition (even before the irradiance peak)  
31 indicate a photoprotective state of PSII.

32  
33 The photoprotective state of HL2 and HL1 cells would also lead to a decreased  
34 photosynthetic efficiency, which is demonstrated by the decrease of  $\alpha^B$ . Since the gradual  
35 PFD increase, cells quickly perform photophysiological regulation processes explaining  
36 both the low value of DPS (<15%) and its efficiency in protecting PSII (see Dimier *et al.*,

1  
2  
3  
4  
5  
6  
7  
8  
9  
10  
11  
12  
13  
14  
15  
16  
17  
18  
19  
20  
2009 a). The highest NPQ value has been reached already under HL1 and no further increase can be observed under HL2 probably in relation to the development of other photoprotective mechanisms such as PSII conformational changes. Additional molecules of Zx under HL2 condition do not have a direct role in NPQ functioning. It is known that Zx molecules are able to indirectly protect PSII through changes in thylakoidal membrane fluidity, or preventing lipid peroxidation (see Goss and Jakob, *in press*). The neoxanthin trend is similar to the one of Zx either over the irradiance range (Fig. 2d) or over the day under HL2 (data not shown). This feature might be related to a role of Neox in preserving PSII from photo-inactivation and protecting membrane lipids as recently demonstrated in plants (Dall'Osto *et al.*, 2007).

21  
22  
23  
24  
25  
26  
27  
28  
29  
30  
31  
32  
33  
34  
35  
36  
37  
38  
39  
40  
41  
42  
43  
44  
45  
46  
47  
48  
49  
50  
51  
52  
This photoprotective status found in cells grown under HL2 might be explained by the rapid kinetics of PFD increase, also linked to the higher irradiance reached, or also by the increase in accessory photosynthetic pigments, which might have enhanced the sensitivity of PSII to high light. The role of photoprotective pigments as a trap for a part of the harvested electrons would thus decrease the quantum yield leading to an energy-deficient state during low light periods that would in turn require an increase in the light-harvesting pigment content. This last hypothesis supposes a feedback-relationship between photoprotection and photoacclimation aiming to enhance the light harvesting capacity of cells. Cells would perceive both high light values and low light dose per day (e.g., through the time spent under low light) and respond to both these factors. Such a special physiological plasticity is likely to occur in species growing in coastal waters where high vertical mixing implies fast shifts between high and low light conditions. This hypothesis agrees with the results obtained by Dimier and co-workers (2009 b) where it has been shown that coastal species are physiologically “intermediary” compared to surface-offshore and deep water species, in terms of both photosynthetic and photoprotective pigment content. Further studies are needed to test this hypothesis and to obtain clearer knowledge on the ecophysiological capacity of coastal phytoplankton, such as many diatoms, to efficiently photoacclimate and photoprotect.

53  
54  
55  
56  
57  
58  
59  
60  
*Phaeomonas sp.* is not able to grow under strong light limitation (e.g., for a  $E_k$  : PFD ratio > 10). The fact that the increase in Chl *a* is not coupled with an increase in photosynthetic accessory pigments might suggest an enhancement in number of PSII

1  
2  
3  
4  
5  
6  
7  
8  
9  
10  
11  
12  
13  
14  
15  
16  
17  
18  
19  
20  
21  
22  
23  
24  
25  
26  
27  
28  
29  
30  
31  
32  
33  
34  
35  
36  
37  
38  
39  
40  
41  
42  
43  
44  
45  
46  
47  
48  
49  
50  
51  
52  
53  
54  
55  
56  
57  
58  
59  
60

reaction centers more than in the size of the light-harvesting complexes, distinctive of a n-type photoacclimation strategy (Six *et al.*, 2008). The heavy nutrient cost for low-light growth required by the n-type photoacclimation strategy and its higher-energy cost (Six *et al.*, 2008) can limit or inhibit growth (Dimier *et al.*, 2009 b).

The same photoacclimation strategy has been observed in other picoeukaryotes, the lagoon ecotype of *Ostreococcus tauri* (Six *et al.*, 2008) and the low-light-adapted *Pelagomonas calceolata* (Dimier *et al.*, 2009 a). The latter (Dimier *et al.*, 2009 a) as well as the present study have shown how some species can develop either the  $\sigma$ - or n-type photoacclimation strategy in relation to the light conditions experienced. The n-type photoacclimation strategy would evolve when daily the PFD dose is very low or when cells spend a long time under low light in order to increase their photochemistry (Dimier *et al.*, 2009 a). This result differs from what was shown by Six *et al.* (2008) in two *Ostreococcus* ecotypes (Six *et al.*, 2008), where the n-type photoacclimation evolved in the lagoon ecotype with decreasing growth irradiance. The inconsistency between these studies could be related to the differences of experimental design, since the present study (as Dimier *et al.*, 2009 a) applied a sinusoidal irradiance regime, while the work done by Six *et al.* (2008) employed a continuous irradiance over the light period. Supporting such a hypothesis, Dimier *et al.* (2009 a) showed that the main factor responsible for developing the n- or  $\sigma$ -type photoacclimation was the frequency of irradiance variation during the daylight period.

The very low-light condition surprisingly induces both NPQ generation and little increase in Zx and Neox. Zx and NPQ formation reveals the development of a trans-thylakoidal proton gradient probably caused by chlororespiration (Goss and Jakob, *in press*, and references therein) or by a putative water-water cycle (Mehler's reaction, Badger *et al.*, 2000). It is noteworthy that Neox has a role against photooxidation and would be particularly active when Mehler's reaction takes place (Dall'Osto *et al.*, 2007).

#### ACKNOWLEDGEMENTS

The authors gratefully acknowledge Ferdinando Tramontano for his help during experiments and HPLC analysis. Enzo Saggiomo and Francesca Margiotta are acknowledged for using the spectrophotometer and the CHN and for sharing the PAM

1  
2  
3 probe. Vasco Giovagnetti acknowledges the SZN for his PhD grant. We would like to  
4 thank Dr. D. Campbell and the other anonymous referee for their comments and helping  
5 suggestions improving the quality of the manuscript.  
6  
7  
8  
9

## 10 REFERENCES

- 11  
12  
13  
14 Badger, M.R., Caemmerer, von, S., Ruuska, S. and Nakano, H. (2000) Electron flow to  
15 oxygen in higher plants and algae: rates and control of direct photoreduction  
16 (Mehler reaction) and rubisco oxygenase. *Phil. Trans. R. Soc. Lond. B*, **355**, 1433-  
17 1446.  
18  
19  
20  
21 Brunet, C., Casotti, R., Vantrepotte, V., Corato, F. and Conversano, F. (2007) Vertical  
22 variability and diel dynamics of picophytoplankton in the Strait of Sicily  
23 (Mediterranean Sea) in summer. *Mar. Ecol. Prog. Ser.*, **346**, 15-26.  
24  
25  
26 Dall'Osto, L., Cazzaniga, S., North, H., Marion-Poll, A. and Bassi, R. (2007) The  
27 *Arabidopsis aba4-1* mutant reveals a specific function for neoxanthin in  
28 protection against photooxidative stress. *The Plant Cell*, **19**, 1048-1064.  
29  
30  
31  
32 Dimier, C., Saviello, G., Tramontano, F. and Brunet, C. (2009b) Comparative  
33 ecophysiology of the xanthophyll cycle in six marine phytoplanktonic species.  
34 *Protist*, **160**, 397-411.  
35  
36  
37 Dimier, C., Brunet, C., Geider, R. and Raven, J.A. (2009a) Growth and photoregulation  
38 dynamics of the picoeukaryote *Pelagomonas calceolata* in fluctuating light.  
39 *Limnol. Oceanogr.*, **54**, 823-836.  
40  
41  
42 Dimier, C., Corato, F., Tramontano, F. and Brunet, C. (2007b) Photoprotection and  
43 xanthophyll cycle activity in three diatoms. *J. Phycol.*, **43**, 937-947.  
44  
45  
46 Dimier, C., Corato, F., Saviello, G. and Brunet, C. (2007a) Photo-physiological  
47 properties of the marine picoeukaryote *Picochlorum RCC237* (Trebouxiophyceae,  
48 Chlorophyta). *J. Phycol.*, **43**, 275-283.  
49  
50  
51 Eilers, P.H.C. and Peeters, J.C.H. (1988) A model for the relationship between light  
52 intensity and the rate of photosynthesis in phytoplankton. *Ecol. Model.* **42**, 199-  
53 215.  
54  
55  
56  
57  
58  
59  
60

- 1  
2  
3 Falkowski, P. (1983) Light-shade adaptation and vertical mixing of marine  
4 phytoplankton: a comparative field study. *J. Mar. Res.*, **41**, 215-237.  
5  
6  
7 Falkowski, P. and Owens, T.G. (1980) Light-shade adaptation: two strategies in marine  
8 phytoplankton. *Plant Physiol.*, **66**, 592-595.  
9  
10  
11 Finazzi, G., Johnson, G. N., Dall'osto, L., Zito, F., Bonente, G., Bassi, R. and Wollman,  
12 F. A. (2006) Non-photochemical quenching of chlorophyll fluorescence in  
13 *Chlamydomonas reinhardtii*. *Biochemistry*, **45**, 1490–1498.  
14  
15  
16 Finkel, Z., Beardall, J., Flynn, K. J., Quigg, A., Rees, T. A. and Raven, J. A. (2010)  
17 Phytoplankton in a changing world: cell size and elemental stoichiometry. *J.*  
18 *Plankton Res.*, **32**, 119-137.  
19  
20  
21 Hedges, J.I. and Stern, J.H. (1984) Carbon and nitrogen determination of carbonate-  
22 containing solids. *Limnol. Oceanogr.*, **29**, 657-663.  
23  
24  
25 Goss, R. and Jakob, T. (2010) Regulation and mechanism of xanthophyll cycle-  
26 dependent photoprotection in algae. *Photosynthesis Res*, in press.  
27  
28  
29 Guillard, R. R. and Ryther, J.H. (1962) Studies of marine planktonic diatoms. I.  
30 *Cyclotella nana* Hustedt and *Detonula confervacea* (Cleve) Gran. *Can. J.*  
31 *Microbiol.*, **8**, 229-38.  
32  
33  
34 Johnsen, G., Sakshaug, E. (1993). Bio-optical characteristics and photoadaptive  
35 responses in the toxic and bloomforming dinoflagellates *Gyrodinium aureolum*,  
36 *Gymnodinium galatheanum*, and two strains of *Prorocentrum minimum*. *J.*  
37 *Phycol.*, **29**, 627-642.  
38  
39  
40 Lavaud, J., Strzepeck, R. F. and Kroth, P.G. (2007) Photoprotection capacity differs  
41 among diatoms: possible consequences on the spatial distribution of diatoms  
42 related to fluctuations in the underwater light climate. *Limnol. Oceanogr.*, **52**,  
43 1188-1194.  
44  
45  
46  
47 Lewis, M. R., Horne, E. P. W., Cullen, J. J., Oakey, N. S. and Platt T. (1984) Turbulent  
48 motions may control phytoplankton photosynthesis in the upper ocean. *Nature*  
49 **311**: 49–50.  
50  
51  
52  
53 Litchman, E. (2000) Growth rate of phytoplankton under fluctuating light. *Freshw. Biol.*,  
54 **44**, 223-235.  
55  
56  
57  
58  
59  
60

- 1  
2  
3 Litchman, E. and Klausmeier, C. A. (2001) Competition of phytoplankton under  
4 fluctuating light. *Am. Nat.*, **157**, 170–87.  
5  
6  
7 MacIntyre, H. L., Kana T. M., and Geider R. J. (2000) The effect of water motion on  
8 short-term rates of photosynthesis by marine phytoplankton. *Trends Plant Sci.*, **5**,  
9 12–17.  
10  
11 MacIntyre, H. L., Kana T. M., Anning T. and Geider R. J. (2002) Photoacclimation of  
12 photosynthesis irradiance response curves and photosynthetic pigments in  
13 microalgae and cyanobacteria. *J. Phycol.*, **38**, 17–38.  
14  
15  
16  
17 Not, F., Massana, R., Latasa, M., Marie, D., Colson, C., Eikrem, W., Pedrós-Alió, C.,  
18 Vaultot, D. and Simon, N. (2005) Late summer community composition and  
19 abundance of photosynthetic picoeukaryotes in Norwegian and Barents Sea.  
20 *Limnol. Oceanogr.*, **50**, 1677–86.  
21  
22  
23  
24 Peek, M. S., Russek, E., Wait, C. D. A. and Forseth I. N. (2002) Physiological response  
25 curve analysis using nonlinear mixed models. *Oecologia*, **132**, 175-180.  
26  
27  
28 Rascher, U. and Nedbal, L. (2006) Dynamics of photosynthesis in fluctuating light. *Curr.*  
29 *Opin. Plant. Biol.*, **9**, 671-678.  
30  
31  
32 Raven, J. A. (1998) The twelfth Tansley lecture. Small is beautiful: the  
33 picophytoplankton. *Funct. Ecol.*, **12**, 503.  
34  
35  
36 Raven, J. A., Finkel, Z. V. and Irwin A. J. (2005) Picophytoplankton: Bottom-up and top-  
37 down controls on ecology and evolution. *Vie Milieu*, **55**, 209–215.  
38  
39  
40  
41  
42  
43  
44  
45  
46  
47  
48  
49  
50  
51  
52  
53  
54  
55  
56  
57  
58  
59  
60  
Rodriguez, F., Chauton, M., Johnsen, G., Andresen, K., Olsen, L. M. and Zapata, M.  
(2006) Photoacclimation in phytoplankton: implications for biomass estimates,  
pigment functionality and chemotaxonomy. *Mar. Biol.*, **148**, 963-971.  
Six, C., Finkel, Z., Rodriguez, F., Marie, D., Partensky, F. and Campbell D. A. (2008)  
Contrasting photoacclimation costs in ecotypes of the marine eukaryote  
picoplankter *Ostreococcus*. *Limnol. Oceanogr.*, **53**, 255-265.

- 1  
2  
3 Six C., Sherrard, R., Lionard M., Roy S., Campbell D.A. (2009) Photosystem II and  
4 pigment dynamics among ecotypes of the Green Alga *Ostreococcus*. *Plant*  
5 *Physiol.*, **151**, 379-390.  
6  
7  
8  
9 Stransky, H., Hager, A. (1970) Das Carotinoidmuster und die verbreitung des  
10 lichtinduzierten Xanthophyllcyclus in verschiedenen Algenklassen. II.  
11 Xanthophyceae. *Arch. Mikrobiol.*, **71**, 164-190.  
12  
13  
14 Timmermans, K. R., van der Wagt, B., Veldhuis, M. J. W., Maatman, A. and de Baar, H.  
15 J. W. (2005) Physiological responses of three species of marine pico-  
16 phytoplankton to ammonium, phosphate, iron and light limitation. *J. Sea Res.*,  
17 **53**, 109–120.  
18  
19  
20  
21 Worden, A. Z. and Not, F. (2008) Ecology and diversity of picoeukaryotes. *Microbial*  
22 *Ecology of the Oceans, Second Edition*, 159-205.  
23  
24  
25 Van Leeuwe, M. A., Sikkelerus, van B., Gieskes W. W. C. and Stefels, J. (2005) Taxon-  
26 specific differences in photoacclimation to fluctuating irradiance in an Antarctic  
27 diatom and a green flagellate. *Mar. Ecol. Prog. Ser.*, **288**, 9-19.  
28  
29  
30 Vaultot, D., Le Gall, F., Marie, D., Guillou, L. and Partensky, F. (2004) The Roscoff  
31 Culture Collection (RCC): a collection dedicated to marine picoplankton. *Nova.*  
32 *Hedwigia* **79**, 49-70.  
33  
34  
35  
36  
37  
38  
39  
40  
41  
42  
43  
44  
45  
46  
47  
48  
49  
50  
51  
52  
53  
54  
55  
56  
57  
58  
59  
60

1  
2  
3  
4  
5  
6  
7  
8  
9  
10  
11  
12  
13  
14  
15  
16  
17  
18  
19  
20  
21  
22  
23  
24  
25  
26  
27  
28  
29  
30  
31  
32  
33  
34  
35  
36  
37  
38  
39  
40  
41  
42  
43  
44  
45  
46  
47  
48  
49  
50  
51  
52  
53  
54  
55  
56  
57  
58  
59  
60

**FIGURE LEGENDS**

**Fig. 1.** (a) The five sinusoidal light regimes applied during the study, with different maximal PFD peaks (10, 50, 100, 250 and 500  $\mu\text{mol photons m}^{-2} \text{s}^{-1}$ , respectively). Arrows indicate sampling. (b) Evolution of growth rate of *Phaeomonas sp.* over the light conditions. Data are the average of three measurements per three days (corresponding to the exponential growth phase for HL and ML conditions), error bars are SD.

**Fig. 2.** Evolution of: chlorophyll *a*  $\text{cell}^{-1}$  expressed in  $10^{-16} \text{ mol Chl } a \text{ cell}^{-1}$  (a), chlorophyll *c*<sub>2</sub>  $\text{cell}^{-1}$  (white dots) and chlorophyll *c*<sub>3</sub>  $\text{cell}^{-1}$  (black dots) expressed in  $10^{-16} \text{ mol pigment cell}^{-1}$  (b), fucoxanthin  $\text{cell}^{-1}$  (white squares), *cis*-fucoxanthin  $\text{cell}^{-1}$  (white triangles) and  $\beta$ -carotene  $\text{cell}^{-1}$  (grey dots) expressed in  $10^{-16} \text{ mol pigment cell}^{-1}$  (c), and neoxanthin  $\text{cell}^{-1}$  content in  $10^{-17} \text{ mol pigment cell}^{-1}$  (d), over the five PFD conditions. Chl *a*, chlorophyll *a*; Chl *c*<sub>2</sub>, chlorophyll *c*<sub>2</sub>; Fuco, fucoxanthin; *cis*-Fuco, *cis*-fucoxanthin;  $\beta$ -Car,  $\beta$ -carotene, Neox, neoxanthin. Data are the average of three measurements per three days (corresponding to the exponential growth phase for HL and ML conditions), error bars are SD.

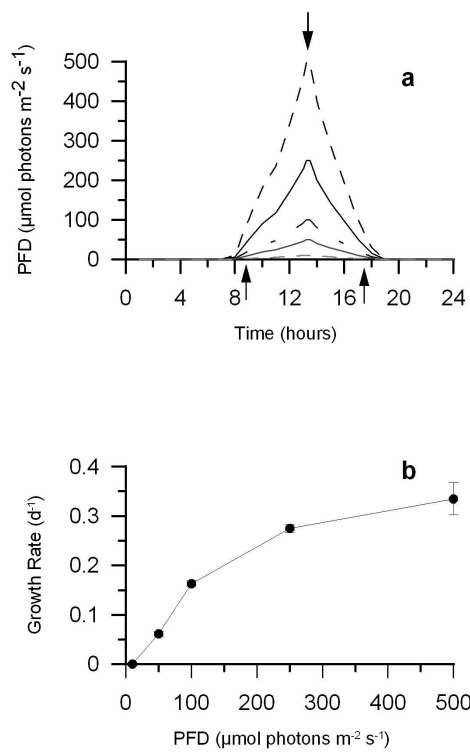
**Fig. 3.** Evolution of: cellular organic carbon (POC, white squares) and nitrogen (PON, black squares) concentrations ( $\text{pg cell}^{-1}$ ) (a), Chl *a* : POC ratio expressed in  $10^{-18} \text{ mol Chl } a^{-1} \text{ pg C}^{-1}$  (b), and POC : PON ratio (c), over the five PFD conditions. Relationship between POC : PON ratio and growth rate ( $r^2 = 98$ ) (d). Data are the average of three measurements per three days (corresponding to the exponential growth phase for HL and ML conditions), error bars are SD.

**Fig. 4.** (a) Evolution of the maximal photosynthetic rate  $\text{absETR}_{\text{max}}$  (in  $\text{mol e}^{-} \text{ g Chl } a^{-1} \text{ h}^{-1}$ ) over the five PFD conditions. Relationship between growth rate and  $\text{absETR}_{\text{max}}$  (b) or  $\text{relETR}_{\text{max}}$  (c). Evolution of  $\alpha^{\text{B}}$  ( $\text{mol e}^{-} \text{ g Chl } a^{-1} \text{ h}^{-1} [\mu\text{mol photons m}^{-2} \text{ s}^{-1}]^{-1}$ , d),  $E_k$  (in

1  
2  
3  $\mu\text{mol photons m}^{-2} \text{ s}^{-1}$ , **e**) and  $E_k$  : PFD ratio (**f**) over the five PFD conditions. Data are the  
4 average of three measurements per three days (corresponding to the exponential growth  
5 phase for HL and ML conditions), error bars are SD.  
6  
7

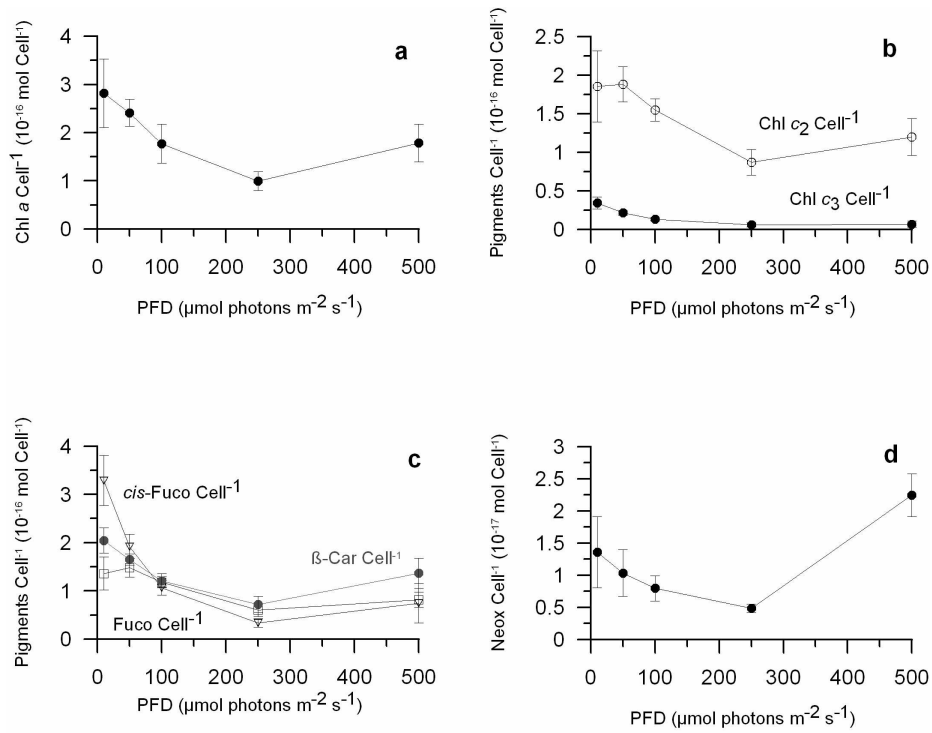
8 **Fig. 5.** Evolution of the maximal photochemical efficiency ( $F_v$  :  $F_m$ ; **a**) and non-  
9 photochemical quenching (NPQ; **b**) over the five PFD conditions. Data are the average of  
10 three measurements per three days (corresponding to the exponential growth phase for  
11 HL and ML conditions), error bars are SD.  
12  
13  
14  
15  
16

17 **Fig. 6. (a)** Relationship between  $Z_x$  : ( $V_x + A_x + Z_x$ ) and NPQ (non-photochemical  
18 quenching). **(b)** Evolution of zeaxanthin  $\text{Chl } a^{-1}$  ( $Z_x \text{ Chl } a^{-1}$  in  $10^{-2} \text{ mol} : \text{mol Chl } a$ ) over  
19 the five PFD conditions. **(c)** Mean of zeaxanthin  $\text{cell}^{-1}$  in the three samples of the dawn,  
20 irradiance peak and sunset under the HL1 and HL2 regimes. Data are the average of three  
21 measurements per three days (corresponding to the exponential growth phase for HL and  
22 ML conditions), error bars are SD.  
23  
24  
25  
26  
27  
28  
29  
30  
31  
32  
33  
34  
35  
36  
37  
38  
39  
40  
41  
42  
43  
44  
45  
46  
47  
48  
49  
50  
51  
52  
53  
54  
55  
56  
57  
58  
59  
60



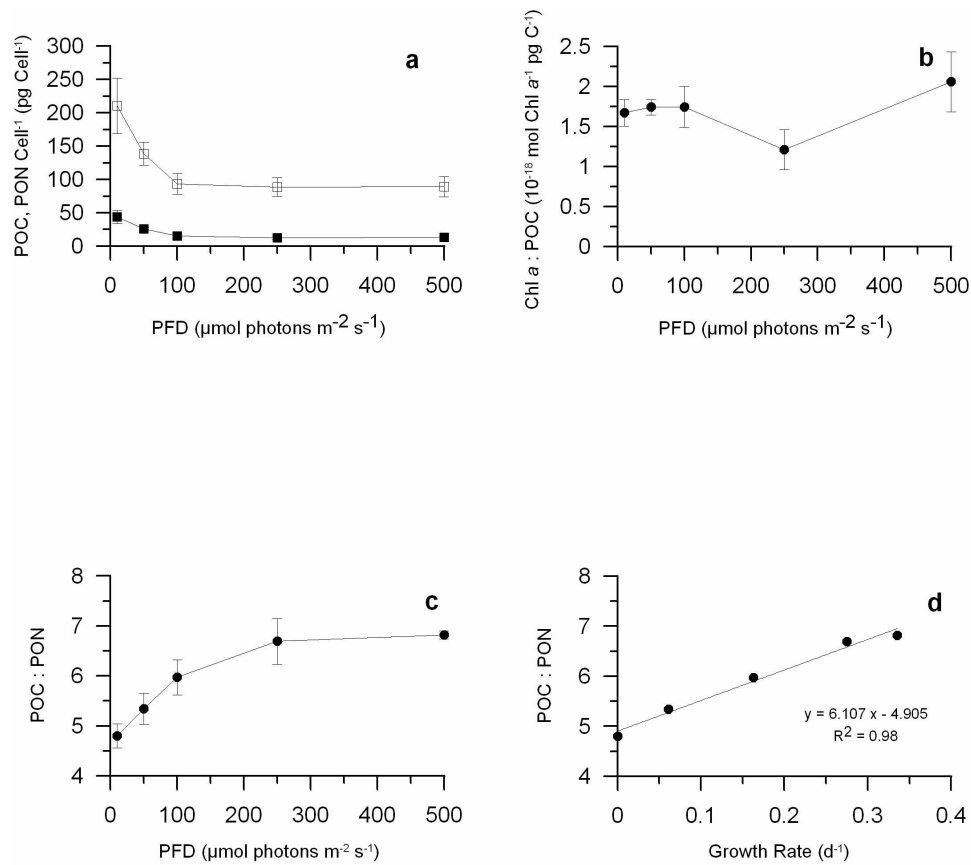
Giovagnetti et al.\_Fig. 1

89x231mm (300 x 300 DPI)



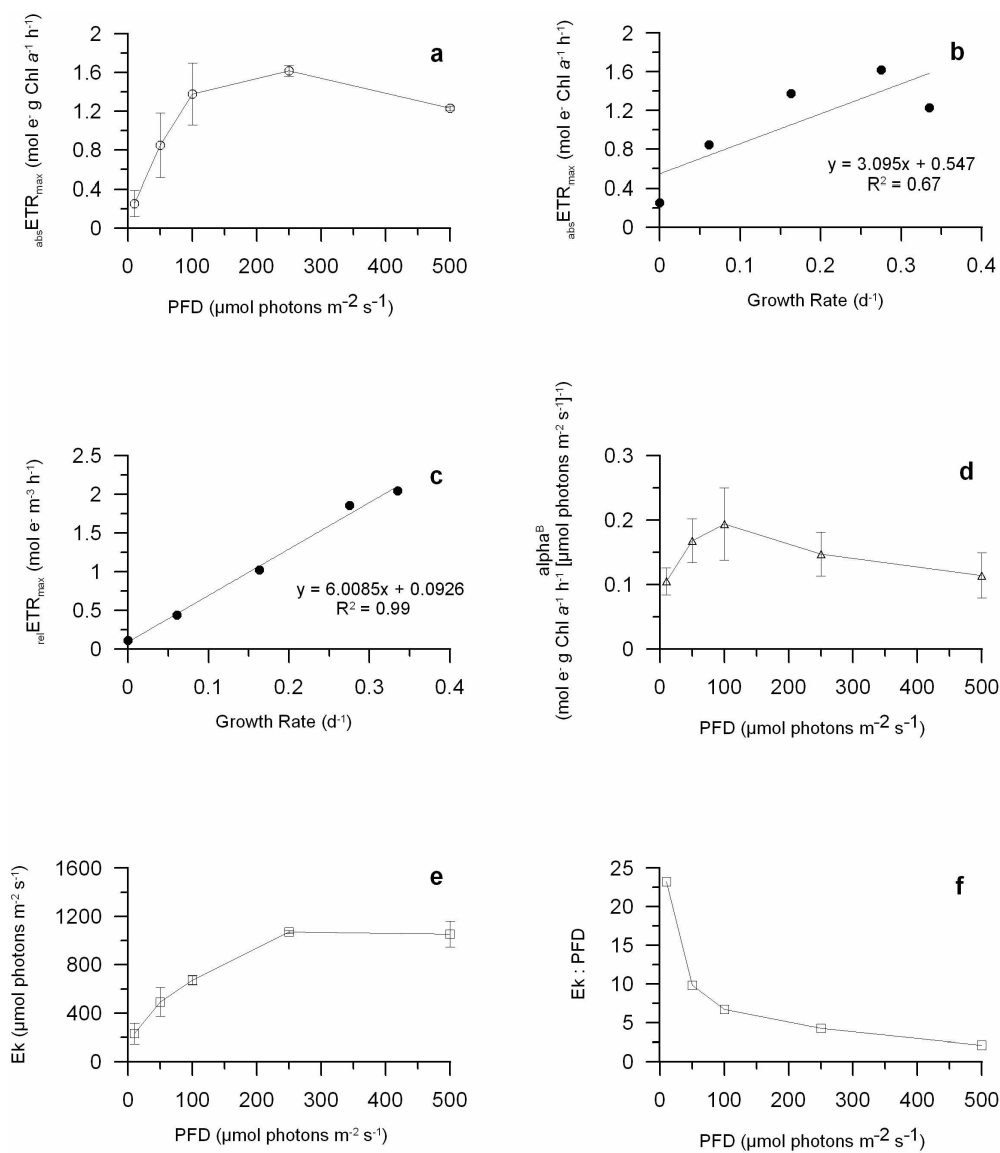
Giovagnetti et al.\_Fig. 2

182x236mm (300 x 300 DPI)



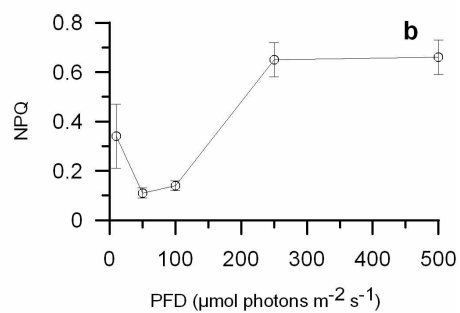
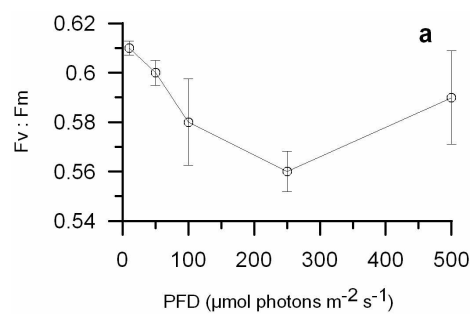
Giovagnetti et al.\_Fig. 3

182x228mm (300 x 300 DPI)



Giovagnetti et al.\_Fig. 4

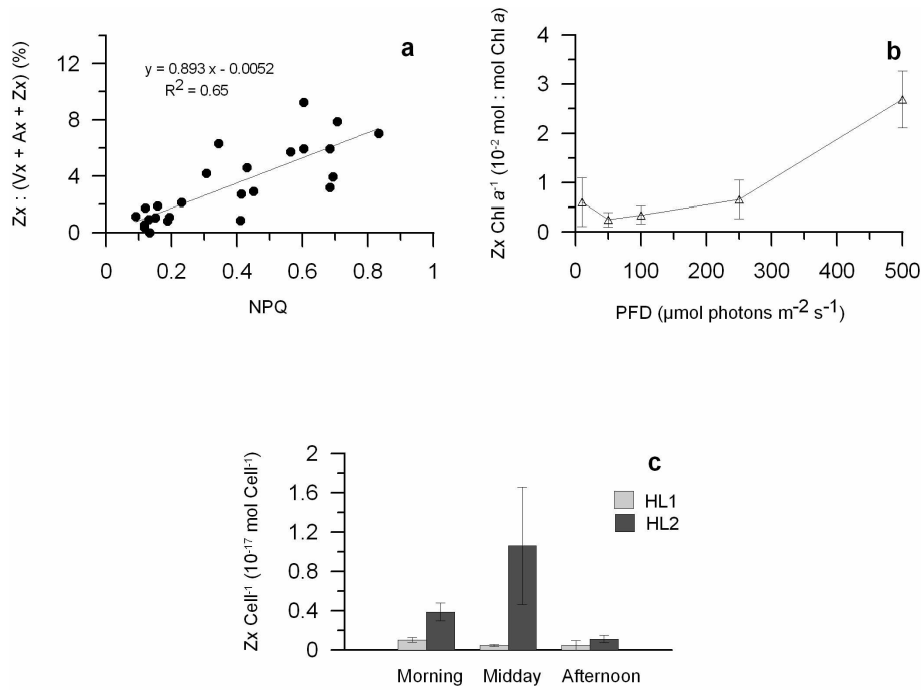
195x236mm (300 x 300 DPI)



46  
47  
48  
49  
50  
51  
52  
53  
54  
55  
56  
57  
58  
59  
60

Giovagnetti et al.\_Fig. 5

88x231mm (300 x 300 DPI)



Giovagnetti et al.\_Fig. 6

176x232mm (300 x 300 DPI)